Talanta 162 (2017) 19–23

Contents lists available at ScienceDirect

Talanta

journal homepage: www.elsevier.com/locate/talanta

Hydrodynamic injection on electrophoresis microchips using an electronic micropipette

Ellen F.M. Gabriel[a], Rodrigo A. dos Santos[a], Eulício O. Lobo-Júnior[a], Kariolanda C.A. Rezende[a], Wendell K.T. Coltro[a,b,*]

[a] Instituto de Química, Universidade Federal de Goiás, 74690-900 Goiânia, GO, Brazil
[b] Instituto Nacional de Ciência e Tecnologia em Bioanalítica (INCTBio), 13083-970 Campinas, SP, Brazil

ARTICLE INFO

Keywords:
Automatic dispensing
Bias-free sample injection
Microfluidic transport
Portable instrumentation

ABSTRACT

Here we report for the first time the use of an electronic micropipette as hydrodynamic (HD) injector for microchip electrophoresis (ME) devices. The micropipette was directly coupled to a PDMS device, which had been fabricated in a simple cross format with two auxiliary channels for sample volume splitting. Sample flow during the injection procedure was controlled in automatic dispenser mode using a volume of 0.6 µL. Channel width and device configuration were optimized and the best results were achieved using a simple cross layout containing two auxiliary channels with 300 µm width for sample splitting. The performance of the HD injector was evaluated using a model mixture of high-mobility cationic species. The results obtained were compared to the data obtained via electrokinetic (EK) injection. Overall, the HD provided better analytical performance in terms of resolution and injection-to-injection repeatability. The relative standard deviation (RSD) values for peak intensities were lower than 5% (n=10) when the micropipette was employed. In comparison with EK injection, the use of the proposed HD injector revealed an unbiased profile for a mixture containing K^+ and Li^+(300 µmol L^{-1} each) over various buffer concentrations. For EK injection, the peak areas decreased from 2.92 ± 0.20–0.72 ± 0.14 V s for K^+ and from 1.30 ± 0.10–0.38 ± 0.10 V s for Li^+ when the running buffer increased from 20 to 50 mmol L^{-1}. For HD injection, the peak areas for K^+ and Li^+ exhibited average values of 2.48 ± 0.07 and 2.10 ± 0.06 V s, respectively. The limits of detection (LDs) for K^+, Na^+ and Li^+ ranged from 18 to 23 µmol L^{-1}. HD injection through an electronic micropipette allows to automatically dispense a bias-free amount of sample inside microchannels with acceptable repeatability. The proposed approach also exhibited instrumental simplicity, portability and minimal microfabrication requirements.

1. Introduction

Due to the advantages associated with high separation efficiency, instrumental simplicity, low sample and reagent consumption, short analysis time, portability and high-throughput capability, microchip electrophoresis (ME) has become increasingly popular in recent years [1–4]. Recent examples of applications showing the separation of pharmaceuticals compounds [5–7], proteins [2,3,8,9] as well as target analytes for genetic [10,11], food [12,13] and environmental analyzes [14,15] have been successfully reported. Despite the advantages previously cited, ME devices still present some problems that affect the quality of electrophoretic separations, once the sample introduction procedure is one of the most important on-chip steps to ensure reliable and reproducible analysis [4,16–18]. However, the control and manipulation of the ideal volume inside the microchannel is one of the instrumental challenges to be overcome. Sample introduction on ME devices can be performed by electrokinetic (EK) or hydrodynamic (HD) modes [17–19]. As well known, in the EK injection, the analytes flow through the microchannel under the application of electrical field. With HD injection, the application of pressure promotes the introduction of a specific volume inside the microchannel [16,20–22].

The applications involving ME devices are often explored through sample EK injection due to its instrumental simplicity [3,20]. However, this kind of injection mode is biased and presents some undesirable features that negatively affect the electrophoretic performance and, consequently, the reliability of the quantitative analysis [16,17]. During the EK injection, the amount of analyte introduced into microchannel is strongly dependent on the electrophoretic mobility as well as the electroosmotic flow (EOF) magnitude. In this way, species with high mobility are preferably injected in comparison with low mobility compounds [16–18,23,24]. In addition to the biased injection, the dependence on sample conductivity, the influence of electrolysis on the

* Corresponding author at: Instituto de Química, Universidade Federal de Goiás Campus Samambaia, 74690-900 Goiânia, GO, Brazil.
E-mail address: wendell@ufg.br (W.K.T. Coltro).

http://dx.doi.org/10.1016/j.talanta.2016.09.046
Received 10 August 2016; Received in revised form 16 September 2016; Accepted 17 September 2016
Available online 20 September 2016
0039-9140/

pH and sample leakage represent other common features to be minimized with the use of EK injection [18,25,26].

Given the limitations of the EK mode, the value of HD injection when using ME devices has received growing attention in recent years [3,16,27]. HD sample introduction has been achieved using hydrostatic, negative and positive pressure [18]. In these examples, the sample introduction and the fluid flow control were realized by micropumps [17,28–30], microvalves [19,21,22,27,31,32] and elastomeric actuators [33–36], which can be positioned inside or outside the microfluidic platform.

Although many HD injection methods have demonstrated good analytical performance to overcome the introduction of a biased sample, most of the reported approaches are laborious and require sophisticated microfabrication facilities, which may not be readily accessible. On the other hand, the use of electronic micropipettes in analytical systems has demonstrated valuable instrumental potentiality due to its capability to realize aspiration, propulsion and sample injection. Examples of applications involving micro-flow [37] and batch injection analysis [38–41] have been successfully reported. In this scenario, this paper describes for the first time the use of an electronic micropipette as HD injector for ME devices. The micropipette tip was directly positioned on the PDMS microchannel using a polymeric tube as connector. In order to reduce the sample volume dispensed by the electronic micropipette, the ME device was designed with two auxiliary channels to promote sample splitting. The proof-of-concept of the proposed injector was demonstrated with the separation of high-mobility cationic species. The HD injector can provide unbiased injections independently of the running buffer concentration.

2. Material and methods

2.1. Chemicals and materials

Decafilm W*R* emulsion (poly(vinyl) acetate, PVAc) and photoinitiator (Diazo D Sensitizer salt) were obtained from Polo Visual (Goiânia, GO, Brazil). Sylgard 184 silicone elastomer and curing agent were acquired from Dow Corning (Midland, MI, USA). Glass slides (24 × 60 × 0.1 mm) were purchased from Protec (Goiânia, GO, Brazil). Sodium chloride, potassium chloride, lithium chloride, L-Histidine (His), 2-(*N*-morpholino) ethanesulfonic acid (MES) were received from Sigma Aldrich (St. Louis, MO, USA). The 20 mmol L^{-1} MES/His running buffer solution (pH 6.1) was prepared weekly in ultrapure water (resistivity ≥18 MΩ). Stock solution of cations (10 mmol L^{-1} each) were prepared from the corresponding chloride salts. All chemicals were reagent grade. Ultrapure water was used throughout.

2.2. Fabrication of PDMS device

PDMS microchannels were fabricated by soft lithography using high-relief masters defined in poly(vinyl acetate), as recently reported [42]. The monomer and the curing agent were mixed at a ratio of 10:1 (m:m), poured on the master, and kept at 80 °C during 30 min. Afterwards, PDMS replica was peeled off the master and sealed against a glass surface previously coated with a PDMS membrane [43], as shown in Fig. 1A. Prior to the curing step, a polymeric tube (0.3 cm) was added on the reservoir dedicated to injection point in order to promote the coupling between electronic micropipette and ME device (Fig. 1B). PDMS electrophoresis devices were fabricated in a simple cross format with two auxiliary channels for sample volume splitting (Fig. 1A). The split, injection and separation channels were 2.5, 2.5 and 45 mm long, respectively. The width of the injection and separation channels were of 50 µm. The width of the split channels was 300 µm. The depth of all channels was approximately 40 µm.

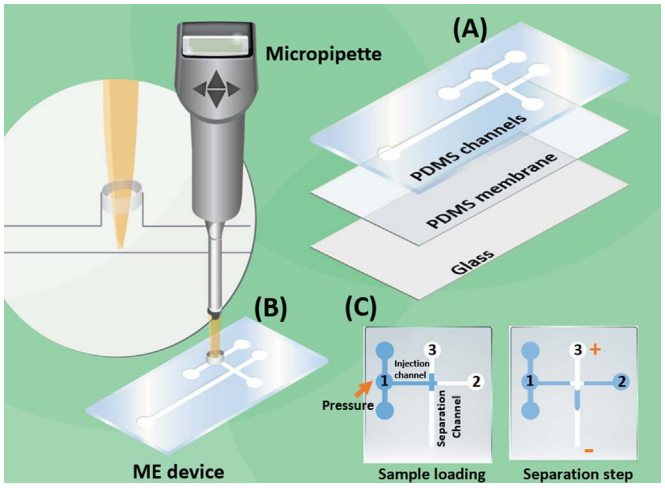

Fig. 1. Scheme of the (A) microfluidic structure arranged in a PDMS/glass platform, (B) coupling between electronic micropipette and PDMS device and (C) sample introduction with volume splitting prior to electrophoretic separation.

2.3. Hydrodynamic injection

To proceed with unbiased injection, the sample was introduced in HD mode. In this step, a commercial electronic micropipette purchased from Transferpette® (Wertheim, Germany) electronic was used to sample flow control. This micropipette can be programmable to dispense fractionated volumes from a total volume of 10 µL. The minimal dispensed volume is 0.5 µL. The micropipette was directly coupled to a PDMS device by a polymeric tube as shown in Fig. 1B. During the injection procedure, the use of an electronic micropipette adjusted in the dispenser mode promotes the introduction of a sample amount inside the microchannel. Due to the large volume, the sample is divided through auxiliary channels and a small fraction reaches the intersection between injection and separation channels (Fig. 1C). Then, when the desirable voltage is applied, a sample zone is introduced inside separation channel.

2.4. Electrophoresis procedure and C^4D measurements

PDMS channels were first filled with isopropyl alcohol to avoid the formation of air bubbles. Running buffer was added to all reservoirs and the channels were electrokinetically preconditioned during 10 min. After the conditioning step, the micropipette containing sample solution was connected to the injection point for proceeding the HD injection. Separation was performed under the application of 800 V. The voltages were generated using a bipolar two-channel high voltage sequencer model ER230 from eDAQ (Denistone East, Australia). Electrophoretic separations were monitored by a lab-made C^4D system developed according to electronics reported by da Silva et al. [44]. C^4D was performed by applying a 400 kHz sinusoidal wave with 1 $V_{peak\text{-}to\text{-}peak}$ amplitude to the excitation electrode. The resulting signal was recorded in a receiver electrode and monitored in real time using a software written in Lab*VIEW*® (National Instruments, Austin, TX, USA). Sensing electrodes were fabricated on office paper sheet by a hand drawing protocol using a graphite pencil as described elsewhere [44]. The electrodes (2-mm wide) were designed in an antiparallel configuration with distance between the electrodes of 1 mm and length of 20 mm.

3. Results and discussion

3.1. Characterization of the hydrodynamic system

The sample amount injected into the separation channel depends

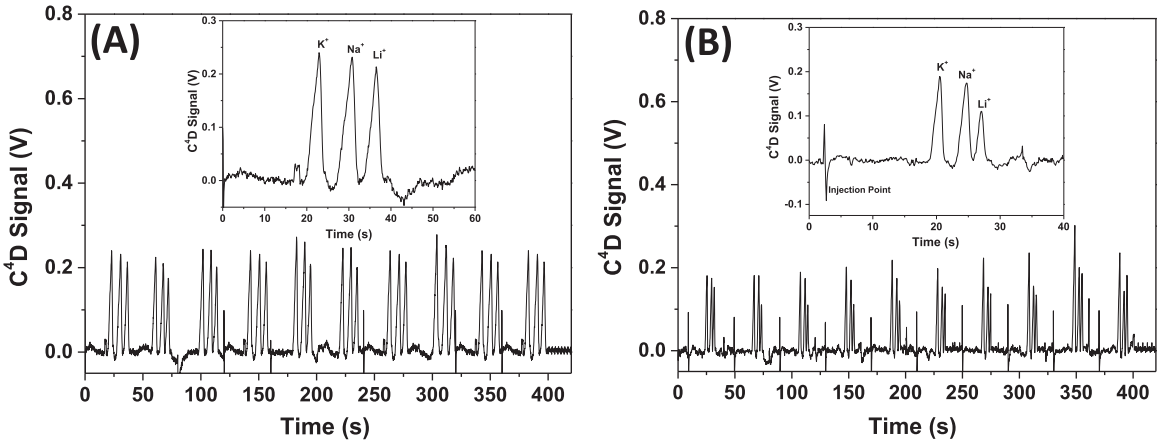

Fig. 2. Electropherograms showing the separation of a model mixture of inorganic cations (K^+, Na^+ and Li^+, 300 μmol L^{-1} each) introduced inside separation channels by (A) HD and (B) EK injection modes. Separation voltage: 800 V. Running buffer: 20 mmol L^{-1} MES/His, pH 6.1. Dispensing rate: 12 ± 1 μL s^{-1}. Detection conditions: 400-kHz, 1.5 V_{pp}.

on several factors, including the volume controlled by the micropipette, coupling between the micropipette and polymeric device and the channel configuration and dimensions.

The volume dispensed by the micropipette can be controlled in dispenser mode. Using this mode, the volume required to completely fill the entire injection channel was estimated to be 0.6 μL (data not shown). After the volume splitting by using auxiliary channels, the sample flows towards the intersection defined by injection and separation channels. In this step, the sample dispersion through the channels is observed while the voltage required for separation is turned off. The dispersion is affected by the time period between the injection and the voltage application. The longer this delay time, the larger the sample zone plug. In this case, the injection procedure exhibits a strong time dependence. For this reason, the time between the injection and the voltage application was carefully controlled to ensure injection-to-injection repeatability.

Taking into account the sample volume previously defined to be dispensed by the micropipette, the device configuration was optimized in order to ensure the control of the injection volume. Basically, two different configurations were studied including a single-T device as well as a chip with split configuration (two auxiliary channels), as demonstrated in Fig. S1, available in the supplementary material. The principle of the split configuration is similar to the split-mode injection usually explored in gas chromatography [45]. Using the 0.6 μL volume, the single-T configuration was firstly tested. The main problem found with this layout is related to bubbles formation inside channels. The bubbles appeared due to the difference of pressure created during the coupling between PDMS chip and micropipette. Besides, during the electrophoresis procedure, the device did not provide separations with acceptable efficiency and resolution (data not shown). For this reason, the feasibility of a device containing two auxiliary channels was investigated (Fig. S1-B in the Supplemental). The injected volume was theoretically estimated according to the methodology proposed by Gaspar et al. [46], whom explored the Hangen–Poiseuille law. The theoretical value was compared to the experimental data obtained based on the microfluidic area filled with a methylene blue solution and analyzed by optical microscopy. Using channels with width equal to 100 μm, the theoretical volume injection was approximately 12 nL. Comparing this result with the experimental volume (584 μm×100 μm×40 μm), the theoretical volume was approximately five times greater than the experimental value. The biggest theoretical volume can be explained since a large amount of dead volume is observed in the injection point between connector and microchannel. This dead volume was not used for theoretical calculations.

In order to demonstrate the capabilities of split mode with regard to sample volume control, the effect of channel width throughout the injection process was studied. The two auxiliary channels were fabricated with widths ranging from 100 to 400 μm. The theoretical and experimental sample volumes obtained versus channel dimension are displayed in Fig. S2. As it can be observed, the width of auxiliary channels has pronounced effects on sample volume. In general, the larger width, the smaller volume to be injected inside the separation channel. The experimental volume values to fill channels with 100 μm and 400 μm of width are equal to 3.0 and 0.77 nL, respectively. This behavior was somehow expected once the increasing of the channel dimension promotes the decreasing on the fluidic resistance. Consequently, the sample flow towards the auxiliary channels is raised. Because larger split channel widths reduce the injection volume, a value of 300 μm was kept as the ideal configuration for the split channel and used for the remaining experiments.

3.2. Injection-to-injection repeatability

Once the microfluidic geometry and injection volume were selected, the performance of the proposed HD injector was evaluated and compared to the data obtained by EK injection. In this study, a mixture containing cationic species (K^+, Na^+ and Li^+, 300 μmol L^{-1} each) was used as model. Fig. 2A and B display electropherograms recorded for ten consecutive injections using HD and EK injection modes, respectively. As can be seen in Fig. 2, all cations were separated within 50 s with good baseline resolution ($R > 1.0$).

The use of HD injection provided excellent run-to-run repeatability. Table 1 (available in the supplemental) depicts an intra-injection comparison with information about migration times, peak height, peak width and symmetry, separation efficiencies and resolution values. According to the presented data, it can be noted that the HD injection through electronic micropipette provided better analytical performance when compared to EK injection. The peak height for K^+, Na^+ and Li^+ were 0.22 ± 0.02, 0.21 ± 0.01 and 0.20 ± 0.01 V, respectively. The relative standard deviation (RSD) values for peak height decreased from 27% to 5% when HD injection was employed instead of EK mode.

3.3. Unbiased sample injection

When the EK mode is used to perform multiple injections, certain factors can negatively affect the analytical reliability and reproducibility [19]. These key factors include the ionic strength and the pH changes promoted by the electrolysis process. Furthermore, since EK injection is extremely dependent on the electrophoretic mobility and EOF magnitude, minimal change on buffer pH or composition can be enough to harm the injection performance [18,19,47]. Huang et al. [47] reported for the first time the effect of buffer resistance on peak area of model species like K^+ and Li^+, which were introduced inside the capillary under EK and HD injection modes. The authors observed that

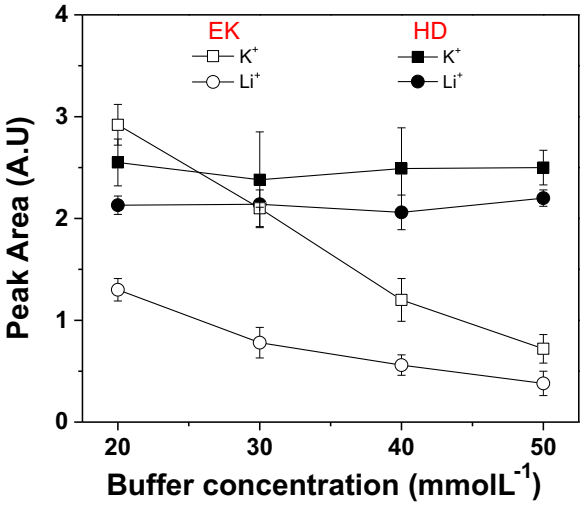

Fig. 3. Effect of running buffer concentration on peak areas for a model mixture (K^+ and Li^+, 300 μmol L^{-1} each) introduced through EK and HD injection modes. HD injection was performed using 0.6 μL; EK injection was performed by floating injection mode (800 V during 10 s). Other conditions: see Fig. 2.

HD injection provides similar peak areas for all conditions, whereas the EK procedure introduces a linear bias, in which a large amount of analytes is injected when buffer solution having higher resistance [47]. Similar results were described by Carneiro et al. [48]. In their study, the peak area for different herbicides decreased when the solution conductivity increased.

Similarly, we evaluated the unbiased sample injection for the proposed HD approach using a mixture of K^+ and Li^+ (300 μmol L^{-1} each) that had previously been prepared in the running buffer to avoid sample preconcentration. The separations were carried out using MES/His running buffer with concentrations ranging from 20 to 50 mmol L^{-1}. As it can be seen in the data depicted in Fig. 3, a decrease in the peak areas for both analytes introduced through EK injection was observed. The peak area values decreased from 2.92 ± 0.20–0.72 ± 0.14 V s and from 1.30 ± 0.10–0.38 ± 0.10 V s for K^+ and Li^+, respectively. The lower amount of injected analyte in higher buffer concentration occurs due to the dependence on electrophoretic mobility and EOF magnitude [47,49]. On the other hand, HD injection promoted the introduction of similar sample amounts independently of the buffer concentration. As presented in Fig. 3, the peak areas for K^+ and Li^+ exhibited average values of 2.48 ± 0.07 and 2.10 ± 0.06 V s, respectively. The results achieved via automatic sample dispensing through as electronic micropipette suggest that sample injection in ME devices was unbiased.

3.4. Analytical performance

Coupling the HD injector to an ME-C^4D system resulted in linear behavior for concentrations ranging from 50 to 250 μmol L^{-1}. The limits of detection (LDs) found for K^+, Na^+ and Li^+ were estimated (S/N=3) to be 18, 20 and 23 μmol L^{-1}, respectively. When compared to the data recorded with the same C^4D electronics, the LD values were similar to those reported for glass [50] and hybrid PDMS/glass [51] devices. However, these values are higher than those reported for polyester-toner [52] and PMMA [44] devices. The main difference was the thickness of the insulation layer between the channel and the electrodes. Herein, the thickness of the insulation was estimated to be approximately150 μm. This layer is probably thicker than the insulation layer used in the references cited [44,52].

4. Conclusions

Here we reported for the first time the use of an electronic micropipette to automatically dispense sample into separation channels by using auxiliary channels for volume splitting. Coupling between microchannel and micropipette does not require laborious microfabrication steps or sophisticated instrumentation. The best experimental conditions were found using a sample volume of 0.6 μL and a microfluidic design in combination with auxiliary channels (300-μm wide) for sample volume splitting. The use of HD injection in combination with the electronic micropipette promoted excellent injection-to-injection repeatability and bias-free sample injection. Similar amounts of K^+ and Li^+ were injected into microchannels when the buffer concentration was changed from 20 to 50 mmol L^{-1}. Furthermore, the proposed HD injector did not compromise the analytical performance recorded with a C^4D system. When the relationship between signal intensity and concentration (50–250 μmol L^{-1} range) was analyzed, linear behavior was observed for all species. The LD values achieved ranged from 18 to 23 μmol L^{-1}; these values are comparable with most previous reports. Notably, the use of an electronic micropipette offers instrumental simplicity and high potentiality for integration with portable equipment for chemical analysis in the field. Due to the low level of energy consumption, the complete set of instrumentation (high-voltage power supply, C^4D system and electronic micropipette) can be powered by batteries or a universal serial bus (USB) port.

Supplementary material

Detailed information about the device configuration, electrophoretic parameters and effect of the split channel dimension on the injection volume.

Acknowledgments

The authors gratefully thank financial support from CNPq (grants 448089/2014-9 and 311744/2013-3), CAPES (grant 3363/2014), FAPEG and INCTBio (573672/2008-3). Lastly, the authors would like to acknowledge Professors Eduardo M. Richter and Claudimir L. do Lago for their suggestions as well as Mr. G. F. Duarte–Júnior for his technical support in the instrumental development.

Appendix A. Supplementary material

Supplementary data associated with this article can be found in the online version at http://dx.doi.org/10.1016/j.talanta.2016.09.046.

References

[1] E.R. Castro, A. Manz, Present state of microchip electrophoresis: State of the art and routine applications, J. Chromatogr. A 1382 (2015) 66–85.
[2] N. Nuchtavorn, W. Suntornsuk, S.M. Lunte, L. Suntornsuk, Recent applications of microchip electrophoresis to biomedical analysis, J. Pharm. Biomed. Anal. 113 (2015) 72–96.
[3] V. Sahore, S. Kumar, C.I. Rogers, J.K. Jensen, M. Sonker, A.T. Woolley, Pressure-actuated microfluidic devices for electrophoretic separation of pre-term birth biomarkers, Anal. Bioanal. Chem. 408 (2015) 599–607.
[4] A. Arora, G. Simone, G.B. Salieb-Beugelaar, J.T. Kim, A. Manz, Latest developments in micro total analysis systems, Anal. Chem. 82 (2010) 4830–4847.
[5] B. Zhang, Z. Chen, Y. Yu, J. Yang, J. Pan, Determination of sulfonamides in pharmaceuticals and rabbit plasma by microchip electrophoresis with LED-IF detection, Chromatographia 76 (2013) 821–829.
[6] A. Fernández-la-Villa, V. Bertrand-Serrador, D.F. Pozo-Ayuso, M. Castaño-Álvarez, Fast and reliable urine analysis using a portable platform based on microfluidic electrophoresis chips with electrochemical detection, Anal. Methods 5 (2013) 1494–1501.
[7] S. Wang, Z. Chen, X. Tang, L. Shi, L. Zhang, M. Yao, Rapid determination of partition coefficients of pharmaceuticals by phase distribution and microchip capillary electrophoresis with contactless conductivity detection, J. Sep. Sci. 36 (2013) 3615–3622.
[8] K.N. Battle, F.I. Uba, S.A. Soper, Microfluidics for the analysis of membrane

proteins: How do we get there?, Electrophoresis 35 (2014) 2253–2266.
[9] W. Ruige, Y. Fung, Microfluidic chip-capillary electrophoresis device for the determination of urinary metabolites and proteins, Bioanalysis 7 (2015) 907–922.
[10] G.H. Hall, D.M. Glerum, C.J. Backhouse, Light emitting diode, photodiode-based fluorescence detection system for DNA analysis with microchip electrophoresis, Electrophoresis 37 (2015) 406–413.
[11] Y.T. Kim, H.Y. Heo, S.H. Oh, S.H. Lee, D.H. Kim, T.S. Seo, Microchip-based forensic short tandem repeat genotyping, Electrophoresis 36 (2015) 1728–1737.
[12] L. Ferey, N. Delaunay, Food analysis on electrophoretic microchips, Sep. Purif. Rev. 45 (2016) 193–226.
[13] E.D. Vega, M.L. Marina, Characterization and study of transgenic cultivars by capillary and microchip electrophoresis, Int. J. Mol. Sci. 15 (2014) 23851–23877.
[14] A.M. Stockton, T.N. Chiesl, J.R. Scherer, R.A. Mathies, Polycyclic aromatic hydrocarbon analysis with the Mars organic analyzer microchip capillary electrophoresis system, Anal. Chem. 81 (2008) 790–796.
[15] C.B. Freitas, R.C. Moreira, M.G. de Oliveira Tavares, W.K. Coltro, Monitoring of nitrite, nitrate, chloride and sulfate in environmental samples using electrophoresis microchips coupled with contactless conductivity detection, Talanta 147 (2016) 335–341.
[16] J.M. Karlinsey, Sample introduction techniques for microchip electrophoresis: a review, Anal. Chim. Acta 725 (2012) 1–13.
[17] N. Dossi, R. Toniolo, S. Susmel, A. Pizzariello, G. Bontempelli, A simple approach to the hydrodynamic injection in microchip electrophoresis with electrochemical detection, Electrophoresis 31 (2010) 2541–2547.
[18] R.M. Saito, W.K.T. Coltro, D.P. de Jesus, Instrumentation design for hydrodynamic sample injection in microchip electrophoresis: a review, Electrophoresis 33 (2012) 2614–2623.
[19] J.M. Karlinsey, J. Monahan, D.J. Marchiarullo, J.P. Ferrance, J.P. Landers, Pressure injection on a valved microdevice for electrophoretic analysis of sub-microliter samples, Anal. Chem. 77 (2005) 3637–3643.
[20] C.-H. Tsai, R.-J. Yang, C.-H. Tai, L.-M. Fu, Numerical simulation of electrokinetic injection techniques in capillary electrophoresis microchips, Electrophoresis 26 (2005) 674–686.
[21] A.J. Gaudry, Y.H. Nai, R.M. Guijt, M.C. Breadmore, Polymeric microchip for the simultaneous determination of anions and cations by hydrodynamic injection using a dual-channel sequential injection microchip electrophoresis system, Anal. Chem. 86 (2014) 3380–3388.
[22] R.T. Kelly, C. Wang, S.J. Rausch, C.S. Lee, K. Tang, Pneumatic microvalve-based hydrodynamic sample injection for high-throughput, quantitative zone electrophoresis in capillaries, Anal. Chem. 86 (2014) 6723–6729.
[23] J.P. Alarie, S.C. Jacobson, J.M. Ramsey, Electrophoretic injection bias in a microchip valving scheme, Electrophoresis 22 (2001) 312–317.
[24] S.C. Jacobson, J.M. Ramsey, Microchip electrophoresis with sample stacking, Electrophoresis 16 (1995) 481–486.
[25] D.P. de Jesus, J.G.A. Brito-Neto, E.M. Richter, L. Angnes, I.G.R. Gutz, C.L. do Lago, Extending the lifetime of the running electrolyte in capillary electrophoresis by using additional compartments for external electrolysis, Anal. Chem. 77 (2005) 607–614.
[26] B.E. Slentz, N.A. Penner, F. Regnier, Sampling BIAS at channel junctions in gated flow injection on chips, Anal. Chem. 74 (2002) 4835–4840.
[27] X. Sun, R.T. Kelly, W.F. Danielson, N. Agrawal, K. Tang, R.D. Smith, Hydrodynamic injection with pneumatic valving for microchip electrophoresis with total analyte utilization, Electrophoresis 32 (2011) 1610–1618.
[28] X. Fu, N. Mavrogiannis, S. Doria, Z. Gagnon, Microfluidic pumping, routing and metering by contactless metal-based electro-osmosis, Lab Chip 15 (2015) 3600–3608.
[29] Z. Zhu, J.J. Lu, M.I.G. Almeida, Q. Pu, S.D. Kolev, S. Liu, A microfabricated electroosmotic pump coupled to a gas-diffusion microchip for flow injection analysis of ammonia, Microchim. Acta 182 (2015) 1063–1070.
[30] J.D. Cooper, K.E. Heppert, M.I. Davies, S.M. Lunte, Evaluation of an osmotic pump for microdialysis sampling in an awake and untethered rat, J. Neurosci. Methods 160 (2007) 269–275.
[31] H. Moriguchi, T. Kawai, Y. Tanaka, Simple bilayer on-chip valves using reversible sealability of PDMS, RSC Adv. 5 (2015) 5237–5243.
[32] M.W. Li, B.H. Huynh, M.K. Hulvey, S.M. Lunte, R.S. Martin, Design and characterization of poly(dimethylsiloxane)-based valves for interfacing continuous-flow sampling to microchip electrophoresis, Anal. Chem. 78 (2006) 1042–1051.
[33] A.L. Bowen, R.S. Martin, Integration of on-chip peristaltic pumps and injection valves with microchip electrophoresis and electrochemical detection, Electrophoresis 31 (2010) 2534–2540.
[34] D. Solignac, M. Gijs, Pressure pulse injection: a powerful alternative to electro-kinetic sample loading in electrophoresis microchips, Anal. Chem. 75 (2003) 1652–1657.
[35] F. Lacharme, M.A. Gijs, Single potential electrophoresis microchip with reduced bias using pressure pulse injection, Electrophoresis 27 (2006) 2924–2932.
[36] M.W. Li, R.S. Martin, Integration of continuous-flow sampling with microchip electrophoresis using poly(dimethylsiloxane)-based valves in a reversibly sealed device, Electrophoresis 28 (2007) 2478–2488.
[37] D. Daniel, I.G. Gutz, Electronic micropipettor: a versatile fluid propulsion and injection device for micro-flow analysis, Anal. Chim. Acta 571 (2006) 218–227.
[38] J. Wang, Z. Taha, Batch injection analysis, Anal. Chem. 63 (1991) 1053–1056.
[39] M.S. Quintino, L. Angnes, Batch injection analysis: an almost unexplored powerful tool, Electroanalysis 16 (2004) 513–523.
[40] C. Brett, A.M.O. Brett, L.C. Mitoseriu, Amperometric batch injection analysis: theoretical aspects of current transients and comparison with wall-jet electrodes in continuous flow, Electroanalysis 7 (1995) 225–229.
[41] E.M. Richter, T.F. Tormin, R.R. Cunha, W.P. Silva, A. Pérez-Junquera, P. Fanjul-Bolado, D. Hernández-Santos, A compact batch injection analysis cell for screen printed electrodes: a portable electrochemical system for on-site analysis, Electroanalysis (2016). http://dx.doi.org/10.1002/elan.201600008.
[42] E.O. Lobo-Júnior, E.F.M. Gabriel, R.A. dos Santos, F.R. de Souza, W.D. Lopes, R.S. Lima, A.L. Gobbi, W.K.T. Coltro, Simple, rapid and, cost-effective fabrication of PDMS electrophoresis microchips using poly(vinyl acetate) as photoresist master, Electrophoresis (2016). http://dx.doi.org/10.1002/elps.201600209.
[43] M. Abdelgawad, M.W. Watson, E.W. Young, J.M. Mudrik, M.D. Ungrin, A.R. Wheeler, Soft lithography: masters on demand, Lab Chip 8 (2008) 1379–1385.
[44] C.L.S. Chagas, L.C. Duarte, E.O. Lobo-Júnior, E. Piccin, N. Dossi, W.K.T. Coltro, Hand drawing of pencil electrodes on paper platforms for contactless conductivity detection of inorganic cations in human tear samples using electrophoresis chips, Electrophoresis 36 (2015) 1837–1844.
[45] J. Lisec, N. Schauer, J. Kopka, L. Willmitzer, A.R. Fernie, Gas chromatography mass spectrometry–based metabolite profiling in plants, Nat. Protoc. 1 (2006) 387–396.
[46] A. Gaspar, P. Koczka, H. Carmona, F. Gomez, Split injection: a simple introduction of subnanoliter sample volumes for chip electrophoresis, Microchem. J. 99 (2011) 180–185.
[47] X. Huang, M.J. Gordon, R.N. Zare, Bias in quantitative capillary zone electrophoresis caused by electrokinetic sample injection, Anal. Chem. 60 (1988) 375–377.
[48] M.C. Carneiro, L. Puignou, M.T. Galceran, Comparison of capillary electrophoresis and reversed-phase ion-pair high-performance liquid chromatography for the determination of paraquat, diquat and difenzoquat, J. Chromatogr. A 669 (1994) 217–224.
[49] D. Baker, Capillary Electrophoresis, New York & John Wiley. John Wiley & Sons, Inc., New York, 1995, p. 244.
[50] T.P. Segato, W.K.T. Coltro, A.L.J. Almeida, M.H.O. Piazetta, A.L. Gobbi, L.H. Mazo, E. Carrilho, A rapid and reliable bonding process for microchip electrophoresis fabricated in glass substrates, Electrophoresis 31 (2010) 2526–2533.
[51] M. Vázquez, C. Frankenfeld, W.K.T. Coltro, E. Carrilho, D. Diamond, S.M. Lunte, Dual contactless conductivity and amperometric detection on hybrid PDMS/glass electrophoresis microchips, Analyst 135 (2010) 96–103.
[52] E.F.M. Gabriel, G.F. Duarte Junior, P.T. Garcia, D.P. de Jesus, W.K.T. Coltro, Polyester-toner electrophoresis microchips with improved analytical performance and extended lifetime, Electrophoresis 33 (2012) 2660–2667.